Available online at www.sciencedirect.com
ScienceDirect
Journal of Photochemistry and Photobiology A: Chemistry 195 (2008) 144–150
Journal of Photochemistry and Photobiology A:Chemistry
www.elsevier.com/locate/jphotochem

Enhanced energy conversion efficiency of TiO_2 electrode modified with WO_3 in dye-sensitized solar cells

Ping Cheng *, Changsheng Deng *, Xiaming Dai, Bing Li, Danian Liu, Jingming Xu

State Key Laboratory of New Ceramics and Fine Processing, Institute of Nuclear & New Energy Technology, Tsinghua University, Beijing 100084, People's Republic of China

Received 15 May 2007; received in revised form 7 September 2007; accepted 26 September 2007
Available online 29 September 2007

Abstract

Nanocrystalline TiO_2 films modified with WO_3 were fabricated by depositing TiO_2 suspension containing small amounts of ammonium tungstate solution. The films were characterized with X-ray photoelectron spectroscopy (XPS), X-ray diffraction (XRD), photoluminescence (PL) spectrum, Brunauer–Emmett–Teller (BET) surface area, zeta potential and transient photovoltage measurements. The results indicated that the modification of WO_3 extremely reduced the surface states of TiO_2 and suppressed charge recombination significantly. Compared with unmodified TiO_2 film, the suppression of the interfacial charge recombination and the increased driving force of electron injection contributed to the improved photovoltaic performance of TiO_2 films modified with WO_3. The power conversion efficiency increased as a function of WO_3 content when its concentration was less than 0.5 wt.%. The highest conversion efficiency was obtained with TiO_2 films modified with 0.5 wt.% WO_3, with an increase of 18% improvement in the conversion efficiency than the blank. However, further increasing amount of WO_3 resulted in a decrease in the photocurrent thus reducing the overall conversion efficiency. The retardation of electron injection by the thicker overlayer of WO_3 together with the decrease of the dye loading was responsible for the loss of the efficiency for cells modified with higher concentrations of WO_3.

Keywords: Titania; Surface modification; Dye-sensitized solar cell; Photovoltaic performance

1. Introduction

Dye-sensitized solar cells (DSCs) based on nanocrystalline semiconductors TiO_2 are of great interest as an alternative to the conventional solar cells because of their low-cost production and high performance [1,2]. After more than one decade's development, the energy conversion efficiency of DSC as high as 11% has been achieved under AM 1.5 simulated solar light [3]. Generally, DSC comprises a dye-sensitized nanocrystalline porous TiO_2 film, interpenetrated by a liquid electrolyte containing an I^-/I_3^- redox couple, and a platinized TCO-coated glass substrate. The heart of the system is a mesoporous TiO_2 film composed of nanometer-sized particles possessing a large specific surface area. The light harvesting ability of the dye adsorbed on the nanoporous film is tremendously increased, leading to an improved efficiency of solar cells. However, an unusual feature of this kind of DSC is the lack of the space charge layer, which separates the injected electrons from the holes in the dye or electrolyte [4–6]. The injected electrons may recombine with oxidized dye molecules or with the oxidized redox couple at the TiO_2/dye/electrolyte interface, which remains one of the major limiting factors for the efficiency of the DSC [7]. It has been reported that the efficiency of DSC can be improved by surface modification of TiO_2 with insulating oxides or high band gap semiconductors to form a blocking layer preventing the charge recombination at the TiO_2/dye/electrolyte interface [8–11]. Meanwhile, the electron injection from the excited state of the dye into the conduction band of TiO_2 can occur by tunnelling through the very thin insulating oxide [12]. So, the thickness of the insulating oxide must be thin enough to allow the passage of electrons by tunnelling, otherwise it will decrease the efficiency of the solar cell. In this paper, we first reported the improvement of the photovoltaic characteristics of dye-sensitized solar cells by surface modification of TiO_2 with WO_3. WO_3 modification reduced the surface trap states of TiO_2,

* Corresponding authors. Tel.: +86 10 89796111; fax: +86 10 62771464.
E-mail addresses: phedra2008@yahoo.com.cn (P. Cheng), changsheng@mail.tsinghua.edu.cn (C. Deng).

1010-6030/$ – see front matter © 2007 Elsevier B.V. All rights reserved.
doi:10.1016/j.jphotochem.2007.09.016

suppressed the charge recombination, and increased the driving force of electron injection, thereby improved its power conversion efficiency. The optimization for conversion efficiency of dye-sensitized solar cells based on WO_3-modified TiO_2 was also presented. The influences of the amount of WO_3 on surface trap states of TiO_2, charge recombination, and the solar cell performance were investigated. The solar cells modified with WO_3 showed an improved power conversion efficiency compared with the blank. The highest conversion efficiency of DSC was obtained for TiO_2 nanoparticles modified with 0.5 wt.% WO_3.

2. Experimental

2.1. Preparation of the TiO_2 films and dye-sensitized solar cells

The dye *cis*-$(SCN)_2$bis-(2,2′-bipyridyl-4,4′-dicarboxylate) ruthenium (N_3) was purchased from Solaronix SA. Titanium(IV) isopropoxide, 4-*tert*-butylpyridine and 1-ethyl-3-methylimidazolium iodide (EMII) were purchased from Aldrich. All the materials were reagent grade and used as received. A TiO_2 colloid was prepared according to published procedures. Titanium(IV) isopropoxide (28.4 g) was slowly added to distilled water (300 mL) and then stirred for 30 min. A white precipitate formed immediately upon addition of the titanium(IV) isopropoxide. The resultant colloid was filtered using a glass frit and washed three times with distilled water. The filter cake was transferred to a Teflon-lined titanium autoclave containing 6 mL of a 0.6 M tetramethylammonium hydroxide solution to form white slurry. Peptization occurred after heating the product at 120 °C for 6 h, whereupon the slurry became a milky liquid. Then the slurry was treated hydrothermally in the autoclave at 200 °C for 16 h and was centrifuged to form precipitate. The precipitate was dispersed in a high-speed stirrer by adding an ethanolic solution of ethylcellulose and anhydrous terpineol. The colloidal paste was prepared by evaporating the ethanol at 50 °C under vacuum to a final TiO_2 content of 20 wt.% and a weight ratio of ethylcellulose:TiO_2 = 0.47. To prepare the TiO_2 film, transparent conductive FTO glass (4 mm thick, 75% transmittance in the visible, 20 Ω/sq.) was completely cleaned. The TiO_2 paste was deposited using a simple doctor blade technique on FTO glass. The thickness and the size of the porous TiO_2 layer were controlled by an adhesive tape. Afterward, the film was heated at 450 °C for 60 min before cooling to room temperature. The thickness of the resulting porous TiO_2 film was about 8 μm. For the preparation of TiO_2 films modified with WO_3, the procedures was similar to the above expect that the ammonium tungstate aqueous solution was added into the precipitate and stirred vigorously before dispersed by terpineol. Four kinds of WO_3-modified TiO_2 films were prepared with various stoichiometric ratios of ammonium tungstate to titanium(IV) isopropoxide to get a weight percentage of WO_3 to TiO_2 ranging from 0.25 wt.% to 2 wt.%. Coloration of TiO_2 was carried out by soaking the film in a dry ethanol containing 2.5×10^{-4} M ruthenium complex for 20 h at room temperature. In order to avoid rehydration of the TiO_2 surface or capillary condensation of water vapor from ambient air inside the nanopores of the film, the dye adsorption was done immediately while the electrode was still hot, i.e., its temperature was *ca.* 80 °C. A sandwich cell was prepared with a second conducting glass coated with platinum film, which was deposited from paste containing hexachloroplatinic acid, ethylcellulose/terpineol by screen printing process. The two electrodes were separated by a surlyn spacer (30 μm thick, DuPont) and sealed up by heating at 150 °C. The redox electrolyte was introduced into the space of inter-electrodes through the two holes predrilled on the back of the counter electrode. The two holes were sealed up using a surlyn film, on which a glass slide was pressed under heat. The redox electrolyte used was 0.1 M LiI, 0.1 M I_2, 0.3 M EMII, 0.1 M guanidinium thiocyanate, and 0.5 M 4-*tert*-butylpyridine in acetonitrile.

2.2. Measurements and analysis methods

XRD patterns were made in a Rigaku D/max-RB diffractometer with Cu Kα radiation over the 2θ ranges of 10–90° to identify the phase structure of samples. The XPS spectra were recorded on a Perkin-Elmer PHI 5000 C ESCA system equipped with a dual X-ray source, of which the Al Kα (1486.6 eV) anode and a hemispherical energy analyzer were used. All binding energies were calibrated using contaminant carbon (C_{1s} = 284.6 eV) as a reference. The films were scraped from the glass substrate and powdered for HRTEM, Nitrogen adsorption–desorption, zeta potentials and photoluminescence (PL) spectra measurements. HRTEM micrographs were obtained on a JEOL JEM-2011 transmission electron microscope. The samples were supported on carbon-coated copper grids for the experiment. The Brunauer–Emmett–Teller (BET) surface area was determined by nitrogen adsorption–desorption isotherm measurements at 77 K on a Micromeritics NOVA 3200e nitrogen adsorption apparatus. The samples were degassed at 300 °C before each measurement. PL spectra were measured at room temperature on a Perkin-Elmer LS55 spectrometer using a 325 nm excitation light. Zeta potential measurements were carried out on BI-ZetaPlus (Brookhaven Instruments Corp., USA), which uses the Doppler shift resulting from laser light scatter from the particles to obtain a mobility spectrum. Samples were prepared at solids concentration of 0.5 wt.% in deionized water, 10^{-3} M NaCl electrolyte, and dispersed for 10 min using an ultrasonic probe. After dispersing, the solution was allowed to sediment for 20 min and the agglomerates were removed. The 10^{-2}N HCl and 10^{-2}N NaOH solutions were used to adjust pH to the desired values. The pH values of the solutions were measured with a pH meter.

For the transient photovoltage study of the DSC, the cells were probed with a weak laser pulse at 532 nm, which was generated by a frequency-doubled Nd:YAG laser (pulse duration 15 ns). The 532 nm probe light was strongly absorbed by the dye and was incident from the front (FTO) side of the DSCs in an effort to make the measurement under real DSCs operating conditions. The transient photovoltage signal was tested under an open circuit condition and recorded by a TDS220 oscilloscope (Tektronix). Current–voltage curves were recorded using

a source meter (Keithley-2400, Keithley Co. Ltd., USA) under an illumination of 100 mW cm^{-2} (globe AM 1.5, 1sun) from a 300 W xenon lamp (Oriel). Incident monochromatic photo-to-current conversion efficiency (IPCE) measurements were carried out using a computer-controlled setup. A 300 W xenon lamp was used as a light source in combination with small band-pass filters (Schott Co.) to generate monochromatic light.

3. Results and discussion

XPS was employed to investigate the chemical valence state and relative quantities of the outermost surface of the films. Fig. 1 shows XPS spectra of Ti 3p region for blank and WO_3-modified TiO_2 films. It can be observed that there is a shoulder near the strongest peak of Ti 3p when the content of WO_3 is above 0.5 wt.%. The intensity of the shoulder increases as a function of the content of WO_3. Based on the Gaussian–Lorentzian function, the spectra with the content of WO_3 above 0.5% can be fitted with two components, one located at 37.1 eV corresponding to Ti 3p, and the other located at 35.2 eV, assigned to W $4f_{7/2}$ [13]. It has been reported that the W $4f_{7/2}$ peak in WO_3 powders or films is located around 35 eV [14,15]. Therefore, the tungsten (W) in the modified TiO_2 films was present in the six-valence state (W^{6+}) in form of WO_3. The weight ratios of WO_3 to TiO_2 were estimated according to the relative peak intensities of W 4f and Ti 2p after correction with atomic sensitivity factors, which were listed in Table 1. It can be observed that the surface WO_3 content was much higher than the stoichiometric ratio as directly mixed, inferring that WO_3 was present on the surface of TiO_2. In order to confirm the morphology of WO_3, HRTEM

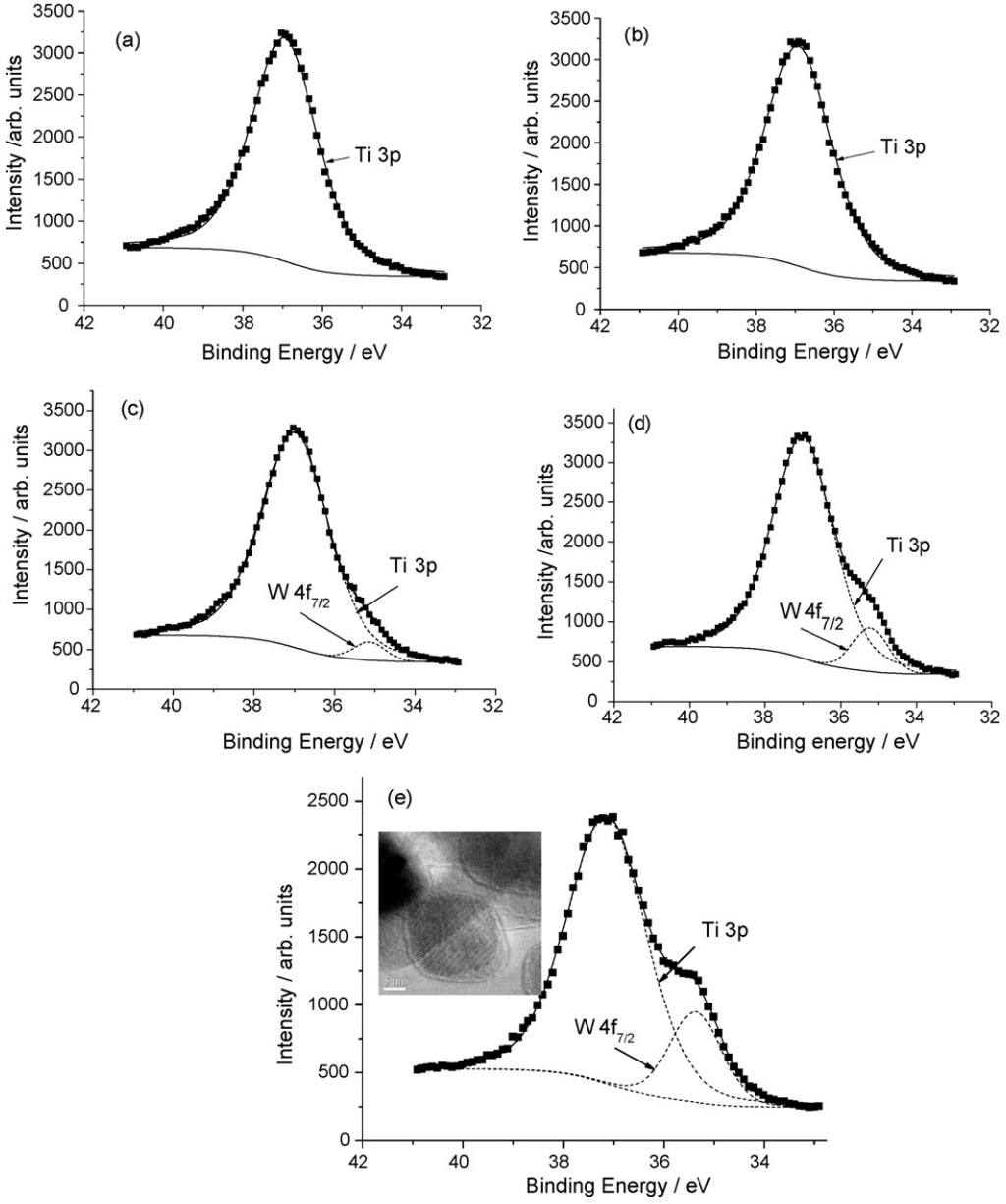

Fig. 1. XPS spectra of the Ti 3p region for TiO_2 films modified with various WO_3 contents: (a) blank, (b) 0.25%, (c) 0.5%, (d) 1% and (e) 2%. The dotted lines are the fitted spectra with Lorentzian–Gaussian curve.

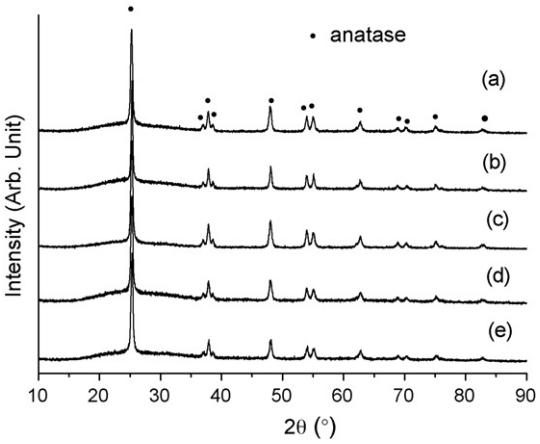

Fig. 2. XRD patterns of TiO_2 films modified with various WO_3 contents: (a) blank, (b) 0.25%, (c) 0.5%, (d) 1% and (e) 2%.

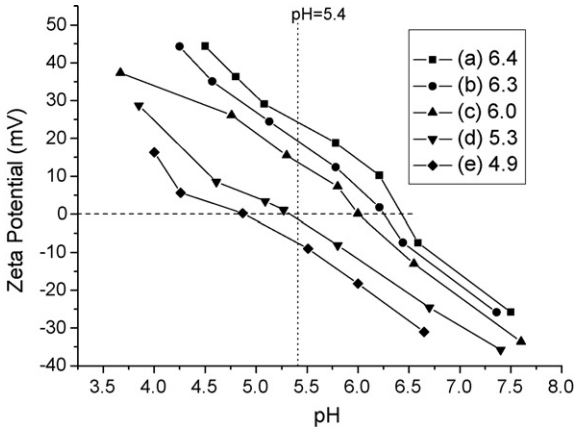

Fig. 3. Zeta potentials of TiO_2 modified with various WO_3 contents: (a) blank, (b) 0.25%, (c) 0.5%, (d) 1% and (e) 2%. The numbers following the parentheses denote the corresponding isoelectric points of the samples.

was employed. No clear coating layer was observed when the content of WO_3 was 0.5%, probably because that the coating was too thin and the size was out of the limit of the equipment. However, the overlayer of WO_3 on the surface of TiO_2 could be clearly observed when the content of WO_3 was 2%, as shown in the inset of Fig. 1e.

Fig. 2 shows XRD patterns of unmodified and WO_3-modified TiO_2 films. It can be observed that, for all the films, there are only diffraction peaks of anatase TiO_2. It indicated that TiO_2 crystalline structure was transformed from amorphous to anatase after heated at 450 °C for 60 min. For the WO_3-modified TiO_2 films, we cannot observe the diffusion peaks of the WO_3 in the XRD patterns probably due to the ultrathinness of the WO_3 layer on the TiO_2. The grain size of anatase TiO_2 was calculated according to the Scherrer formula. The estimated grain size as well as BET surface area was listed in Table 1. It can be seen that WO_3 modification had no significant influence on the grain size and specific surface area of TiO_2 nanoparticles.

Generally, for a given dye, the amount of dye adsorbed on TiO_2 is correlated with the specific surface area of TiO_2. Quantitative analysis was done by desorbing dye molecules from presoaked TiO_2 film into a solution of 10^{-4} M NaOH in ethanol and measuring its absorption spectrum. The amount of the adsorbed dye on TiO_2 was also listed in Table 1. It can be observed that the amount of the adsorbed dye decreases with the increase of the WO_3 content, especially when the WO_3 content is above 0.5%. For example, for TiO_2 modified with 2% WO_3, the amount of the adsorbed dye decreases by 7.8%, while its specific surface area decreases only by 0.5% compared to that of unmodified TiO_2 (Table 1). So the specific surface area was not mainly responsible for the decrease of the dye adsorption. In order to clarify the reason that a less dye uptake was obtained for WO_3-modified TiO_2, zeta potentials of the TiO_2 particles modified with various WO_3 contents were measured.

Table 1
Characteristics of unmodified and WO_3-modified TiO_2

	Stoichiometric ratio of WO_3 to TiO_2 (wt.%)				
	Blank	0.25	0.5	1	2
WO_3/TiO_2 (wt.%)[a]	0	–	0.81	2.4	4.2
Grain size (nm)	19.0	19.2	19.1	18.9	19.0
A_{BET} ($m^2\,g^{-1}$)[b]	52.09	52.02	52.07	52.14	51.81
Amount of adsorbed dye (10^{-8} mol cm^{-2})	1.28	1.27	1.25	1.21	1.18

[a] Calculated according to the XPS results; wt.% denoted the weight percentage of WO_3 to TiO_2.
[b] BET specific surface area.

Fig. 3 shows the zeta potentials of TiO_2 modified with various WO_3 contents. The results show a clear difference in isoelectric point (IEP) between the samples. For unmodified TiO_2 and TiO_2 modified with 0.25%, 0.5%, 1% and 2% of WO_3, the isoelectric point is 6.4, 6.3, 6.0, 5.3 and 4.9 pH units, respectively. It can be clearly observed that the IEP of the particles shifts to lower pH values with the increase of WO_3 content. For a given curve, when independent variable of pH is less than the IEP, the zeta potential for the sample is above the horizontal axis, which means that the surface of TiO_2 nanoparticles is of positive charge. The natural pH value for the dye in ethanol solution is 5.4. Therefore, for blank TiO_2, 0.25%WO_3/TiO_2 and 0.5%WO_3/TiO_2 particles, the pH value of the dye solution is smaller than the IEP, and the surface of TiO_2 particles is positively charged. However, for 1%WO_3/TiO_2 and 2%WO_3/TiO_2, the pH of the dye solution is larger than the IEP, and a negative zeta potential is obtained, which implies the surface of TiO_2 particles is negatively charged. As a result, for blank TiO_2, 0.25%WO_3/TiO_2 and 0.5%WO_3/TiO_2 nanoparticles, the positively charged TiO_2 offers a favorable surface for the adsorption of electronegative N_3 dye molecules. However, for 1%WO_3/TiO_2 and 2%WO_3/TiO_2, there exists an electrostatic repulsion between the electronegative N_3 dye molecules and negatively charged TiO_2 surface, which is adverse to the adsorption of dye molecules onto TiO_2 surface. So the isoelectric point is responsible for the decrease of the dye adsorption for WO_3-modified TiO_2.

It has been reported that there are a large number of surface states in nanocrystalline TiO_2, which are energetically located below the TiO_2 conduction band with an exponential distribution

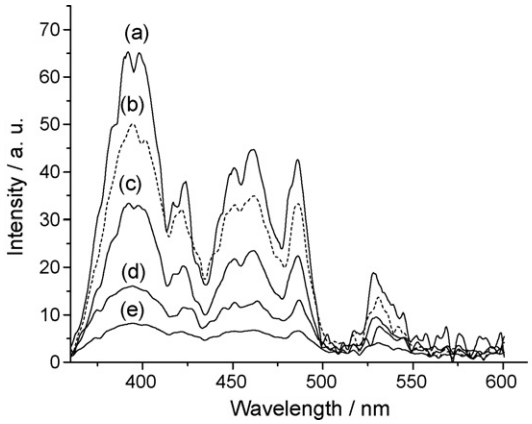

Fig. 4. The photoluminescence spectra of TiO_2 films modified with various WO_3 contents: (a) blank, (b) 0.25%, (c) 0.5%, (d) 1% and (e) 2%.

[16,17]. The recombination between the injected electrons and the oxidized redox couple or dye molecules occurs principally via trap states rather than via the conduction band [18,19]. So, these surface states are deleterious to the performance of DSC since they can trap carriers and promote their recombination. The PL emission spectra were investigated to explore the change of surface states of TiO_2. Fig. 4 shows the comparison of the room temperature photoluminescence spectra for blank TiO_2 and TiO_2 modified with various WO_3 contents. For blank TiO_2 (Fig. 5a), the well-resolved peaks/shoulders at 392 nm, 398 nm, 424 nm, 451 nm, 461 nm, 486 nm, and 528 nm were observed. All these peaks/shoulders are ascribed to surface traps [20–22]. A similar PL spectrum was reported by Serpone et al. for TiO_2 ultrafine particles prepared by controlled hydrolysis of titanium butoxide [23,24]. It can be seen from Fig. 4 that WO_3-modified TiO_2 samples show a significant decrease in the intensity of PL spectra compared with unmodified TiO_2. The PL intensity decreases as a function of WO_3 content, indicating the decrease in trap states on surface of TiO_2 nanoparticles. The decrease of the surface states is supposed to be helpful for obtaining high-performance DSCs.

We employed the decay of the transient open-circuit photovoltage following pulsed laser excitation of the sensitized films in the presence of redox active electrolyte to assess the retardation effect of the overlayer of WO_3 for interfacial charge recombination. Fig. 5 compares the transient photovoltage decay of DSCs based on blank TiO_2 and WO_3-modified TiO_2 electrodes. The photovoltage have been normalized to the same peak height at time zero. The decay curve of the photovoltage gives a representation of the charge recombination rate [25,26]. As shown in Fig. 5, the decay time significantly increases with the increase of WO_3 content. It indicates that the WO_3 modification is most effective at retarding the interfacial charge recombination, which is most likely attributed to the decrease in the surface states of TiO_2 as well as the energy barrier formed by WO_3 layer on the TiO_2 surface.

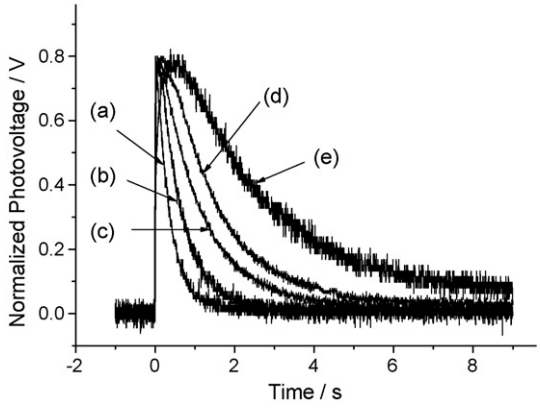

Fig. 5. Normalized transient open-circuit photovoltages for DSCs based on TiO_2 films modified with various WO_3 contents: (a) blank, (b) 0.25%, (c) 0.5%, (d) 1% and (e) 2%.

The current–voltage curves of dye-sensitized solar cells based on TiO_2 films modified with various WO_3 contents are shown in Fig. 6. The corresponding photovoltaic parameters of DSCs are summarized in Table 2. The inset shows the corresponding dark *I–V* characteristics of DSCs. The dark current decreases as a function of WO_3 content, which confirmed the previous discussion about the blocking effect of WO_3 modification for charge recombination shown in Fig. 5. It can be seen from Table 2 that the content of WO_3 has different effects on the open-circuit voltage (V_{oc}), the short circuit photocurrent density (I_{sc}) and the overall conversion efficiency (η). The open-circuit voltage of DSC increases as a function of WO_3 content. For TiO_2 modified with 2%WO_3, V_{oc} increases by 37 mV compared with the unmodified TiO_2. According to diode equation [27], the open-circuit voltage is in inverse proportion to the dark current. So, for

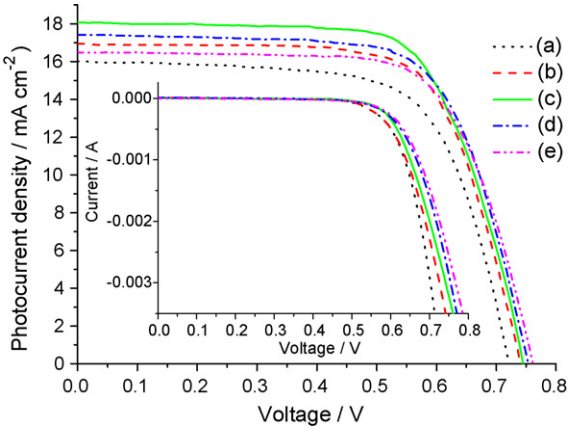

Fig. 6. Current–voltage curves of solar cells obtained using TiO_2 films modified with different WO_3 contents: (a) blank, (b) 0.25%, (c) 0.5%, (d) 1% and (e) 2%. All the films have a size of 1 cm^2 and an illuminating area of 0.533 cm^2. The inset shows the corresponding dark *I–V* curves of DSCs.

Table 2
Photovoltaic characteristics of the DSCs based on the blank TiO_2 and WO_3-modified TiO_2 electrodes

WO_3 ratios (wt.%)	I_{sc} (mA cm^{-2})	V_{oc} (V)	FF	η (%)
0	16.005	0.724	0.67	7.82
0.25	16.944	0.740	0.70	8.77
0.5	18.073	0.745	0.69	9.23
1	17.425	0.753	0.69	8.99
2	16.493	0.761	0.69	8.67

WO_3-modified TiO_2 films, the increase of V_{oc} results from the decrease of the dark current due to the suppressed charge recombination. However, the influence of WO_3 modification on the short circuit photocurrent depends on the content of WO_3. When WO_3 content is less than 0.5%, the short circuit photocurrent increases as a function of WO_3 content and has a maximum value for solar cell modified with 0.5% WO_3. But the I_{sc} decreases for cells modified with higher amount of WO_3 (Table 1). The WO_3 content dependence of the overall conversion efficiency (η) shows the same trend with the short circuit photocurrent. The conversion efficiency (η) increases as a function of WO_3 content when the content of WO_3 is less than 0.5%. The best performance was obtained with TiO_2 film modified with 0.5% of WO_3, with an increase of 18% improvement in conversion efficiency compared with the blank. However, higher concentrations of WO_3 (1% and 2%) reduced the solar cell performance.

The overall photocurrent measured with a solar simulator can also be calculated by convolution of the IPCE values with the AM 1.5 solar spectrum and subsequent integration over the entire spectrum. To analyze in more detail the effect of WO_3 modification on the photocurrent, IPCE measurements have been conducted. Generally, the IPCE of a solar cell is influenced by three factors and the relation between them is described by the following equation [28]:

$$\mathrm{IPCE}(\lambda) = \mathrm{LHE}(\lambda) \times \varphi_{\mathrm{inj}} \times \eta_{\mathrm{coll}}$$

where LHE(λ) is the light harvesting efficiency the colored TiO_2 film, Φ_{inj} is injection efficiency of electron from the excited dye into the conduction band of TiO_2, and η_{coll} is the collection efficiency of the injected electrons by the TCO. For the presented experiments with the same dye as well as the same thickness of nanostructured TiO_2 films, LHE is correlated to dye loading, φ_{inj} is correlated to the conduction band potential of TiO_2 and the oxidation potential of the excited dye, and η_{coll} can be estimated in terms of rates for transport (K_t) and recombination (K_r) in the following way: $\eta_{coll} \propto K_t/(K_t + K_r)$ [29]. In the following study, the observed change in IPCE after WO_3 modification has been investigated by analysis of these factors.

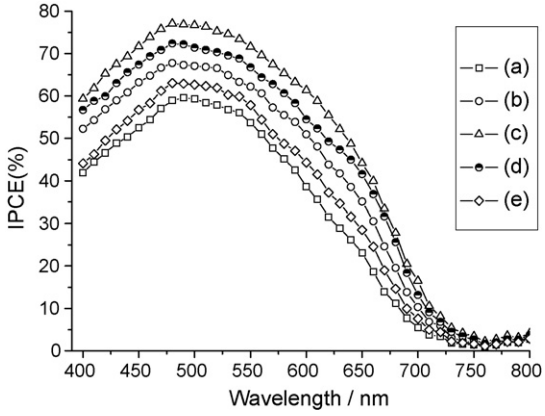

Fig. 7. Photocurrent action spectra of DSCs fabricated from TiO_2 films modified with various contents of WO_3: (a) blank, (b) 0.25%, (c) 0.5%, (d) 1% and (e) 2%.

Fig. 7 shows the IPCE as a function of illumination wavelength for cells obtained by using TiO_2 films modified with different amounts of WO_3. It can be seen that IPCE shows an upward shift as a function of WO_3 content when the content of WO_3 is less than 0.5%. The cell modified with 0.5% WO_3 shows a maximum IPCE of 0.77 at 480 nm, which is much higher than the blank. However, IPCE decreases as a function of WO_3 content at higher amounts of WO_3 (1% and 2%).

As mentioned in Table 1, the amount of the dye adsorbed shows a slight decrease with the increase of WO_3 content, which will result in the decrease of the light harvesting efficiency (LHE). So the increase of the IPCE values upon WO_3 modification (<0.5%) in Fig. 7 must be attributed to the improved collection efficiency (φ_{inj}) or injection efficiency (η_{coll}). Fig. 4 shows that WO_3 modification results in the decrease of surface trap states, which will lead to the suppressed charge recombination as well as the improved transport rate [26], both of which contribute to the increase of the charge collection efficiency. Furthermore, it has been reported that the conduction band of WO_3 is positive than that of TiO_2 (versus normal hydrogen electrode at pH 0) [30]. The modification of WO_3 resulted in a downward shift in the conduction band of TiO_2. The downward shift of the conduction band increased the driving force of the photogenerated electrons transfer from the excited dye to the conduction band of the TiO_2, thus improving the electron injection efficiency [31,32]. Therefore, the improved collection efficiency and injection efficiency due to WO_3 modification are responsible for the increase of the IPCE when WO_3 content is less than 0.5%. It may be noted that a downward shift in the conduction band should give a lower V_{oc}. This does not occur because this effect can be compensated by the reduction of back-reaction current resulting from the retardation of charge recombination.

For cells modified with higher amounts of WO_3 (1% and 2%), the decrease of IPCE is ascribed to the decrease of dye loading or the blocking effect of the thicker WO_3 layer on the electron injection from the excited state of the dye to the conduction band of TiO_2. As mentioned in Table 1 and Fig. 3, WO_3-modified TiO_2 shows a significant decrease in the amount of the adsorbed dye due to the electrostatic repulsion when the WO_3 content is above 0.5%. The decrease of dye loading results in the decrease of the light harvesting efficiency, which leads to the decrease of IPCE. Compared with the blank, the films modified with 1% and 2% WO_3 show the decrease of 3.2% and 5.6% in dye loading, respectively. However, the data in Table 2 show that the loss in short circuit photocurrent is 3.5% and 8.5% for the cells modified with 1% and 2% WO_3, respectively. It is obvious that the decrease in dye loading is partly responsible for the loss of short circuit photocurrent. So the retardation of electron injection due to the thicker WO_3 layer is also probably responsible for the decrease of photocurrent. Although WO_3 modification reduces the surface states or forms a blocking layer between the dye sensitizer and the TiO_2 surface thus suppressing the charge recombination effectively, the thickness of the overlayer must be thin enough to allow the passage of electrons by tunnelling, otherwise it would simultaneously retard the electron injection from the excited state of the dye into the conduction band of TiO_2 thus decreasing the cells IPCE. According to the results

in Fig. 7, 0.5% WO_3 is corresponding to an estimated thickness of 0.02 nm [33], a reasonable thickness in our study, which can both suppress the charge recombination efficiently and allow the electron injection from the excited state of the dye to the conduction band of TiO_2 by tunnelling. However, for the thicker overlayer of WO_3 (1% and 2%), the electron injection from the excited state of the dye into the conduction band of TiO_2 is also suppressed resulting in the decrease of IPCE. So the cell modified with 0.5% WO_3 shows the highest I_{sc} hence the highest overall conversion efficiency under solar illumination (Table 2).

In summary, when the content of WO_3 is less than 0.5%, the increase of the IPCE as a function WO_3 content is attributed to the improved collection efficiency and injection efficiency. Whereas, the decrease of IPCE at higher contents of WO_3 (1% and 2%) results from the decrease of dye loading and the retardation of the electron injection from the excited state of the dye to the conduction band of TiO_2.

4. Conclusion

Dye-sensitized solar cells fabricated from TiO_2 films modified with various concentrations of WO_3 were prepared by depositing TiO_2 suspension containing small amounts of ammonium tungstate solution, which exhibited improved conversion efficiencies compared to unmodified TiO_2 film. The modification of WO_3 reduced the surface states of TiO_2, suppressed the interfacial charge recombination, and increased the driving force of the electron injection, resulting in an increase in open-circuit voltage and short circuit photocurrent compared to the blank. The highest conversion efficiency was obtained with TiO_2 films modified with 0.5 wt.% of WO_3, corresponding to a uniform coverage of 0.02 nm on TiO_2 nanoparticles, with an increase of 18% improvement in the conversion efficiency than the blank. However, for the thicker overlayer of WO_3, electron injection from the excited state of the dye into the conduction band of TiO_2 was also suppressed simultaneously. The retardation of electron injection together with the decrease of the dye loading was responsible for the reduction of the conversion efficiency for cells modified with higher concentrations of WO_3.

Acknowledgments

The authors acknowledge financial support from Institute of Nuclear & New Energy Technology of Tsinghua University, China Postdoctoral Science Foundation, Key Laboratory of New Ceramics and Fine Processing of China.

References

[1] B. O'Regan, M. Gratzel, Nature 353 (1991) 737.
[2] M. Gratzel, Prog. Photovoltaics: Res. Appl. 14 (2006) 429.
[3] M. Gratzel, Inorg. Chem. 44 (2005) 6841.
[4] S. Chappel, S.G. Chen, A. Zaban, Langmuir 18 (2002) 3336.
[5] D. Cahen, G. Hodes, M. Gratzel, J.F. Guillemoles, I. Riess, J. Phys. Chem. B 104 (2000) 2053.
[6] L. Kavan, M. Gratzel, S.E. Gilbert, C. Klemenz, H.J. Scheel, J. Am. Chem. Soc. 118 (1996) 6716.
[7] S. Kambe, S. Nakade, T. Kitamura, Y. Wada, S. Yanagida, J. Phys. Chem. B 106 (2002) 2967.
[8] H. Alarcon, G. Boschloo, P. Mendoza, J.L. Solis, A. Hagfeldt, J. Phys. Chem. B 109 (2005) 18483.
[9] S.G. Chen, S. Chappel, Y. Diamant, A. Zaban, Chem. Mater. 13 (2001) 4629.
[10] Z.-S. Wang, C.-H. Huang, Y.-Y. Huang, Y.-J. Hou, P.-H. Xie, B.-W. Zhang, H.-M. Cheng, Chem. Mater. 13 (2001) 678.
[11] H.S. Jung, J.K. Lee, M. Nastasi, S.W. Lee, J.Y. Kim, J.S. Park, K.S. Hong, H. Shin, Langmuir 21 (2005) 10332.
[12] E. Palomares, J.N. Clifford, S.A. Haque, T. Luz, J.R. Durrant, J. Am. Chem. Soc. 125 (2003) 475.
[13] R. Sivakumar, R. Gopalakrishnan, M. Jayachandran, C. Sanjeevirajal, Smart Mater. Struct. 15 (2006) 877.
[14] J.N. Yao, P. Chen, A. Fujishima, J. Electroanal. Chem. 406 (1996) 223.
[15] L.Y. Su, H. Wang, Z.H. Lu, Mater. Chem. Phys. 56 (1998) 266.
[16] J.E. Kroeze, T.J. Savenije, J.M. Warman, J. Am. Chem. Soc. 126 (2004) 7608.
[17] S.A. Haque, Y. Tachibana, R.L. Willis, J.E. Moser, M. Gratzel, D.R. Klug, J.R. Durrant, J. Phys. Chem. B 104 (2000) 538.
[18] G. Schlichthorl, S.Y. Huang, J. Sprague, A.J. Frank, J. Phys. Chem. B 101 (1997) 8141.
[19] J. Van de Lagemaat, N.-G. Park, A.J. Frank, J. Phys. Chem. B 104 (2000) 2044.
[20] T. Toyoda, T. Hayakawa, K. Abe, T. Shigenari, Q. Shen, J. Lumin. 87–89 (2000) 1237.
[21] F.B. Li, X.Z. Li, Appl. Catal. A 228 (2002) 15.
[22] B.S. Liu, X.J. Zhao, L.P. Wen, Mater. Sci. Eng. B 134 (2006) 27.
[23] N. Serpone, D. Lawless, R. Khairutdinov, J. Phys. Chem. 99 (1995) 16646.
[24] N.D. Abazovic, M.I. Comor, M.D. Dramicanin, D.J. Jovanovic, S.P. Ahrenkiel, J.M. Nedeljkovic, J. Phys. Chem. B 110 (2006) 25366.
[25] P. Wang, L.D. Wang, B.B. Ma, B. Li, Y. Qiu, J. Phys. Chem. B 110 (2006) 14406.
[26] N. Kopidakis, K.D. Benkstein, J. Van de Lagemaat, A.J. Frank, J. Phys. Chem. B 107 (2003) 11307.
[27] M. Gratzel, J. Photochem. Photobiol. A: Chem. 164 (2004) 3.
[28] M.K. Nazeeruddin, A. Kay, I. Rodicio, R. Humpry-Baker, E. Muller, P. Liska, N. Vlachopoulos, M. Gratzel, J. Am. Chem. Soc. 115 (1993) 6382.
[29] P.M. Sommeling, B.C. O'Regan, R.R. Haswell, H.J.P. Smit, N.J. Bakker, J.J.T. Smits, J.M. Kroon, J.A.M. van Roosmalen, J. Phys. Chem. B 110 (2006) 19191.
[30] M. Miyauchi, A. Nakajima, K. Hashimoto, T. Watanabe, Adv. Mater. 12 (24) (2000) 1923.
[31] G. Boschloo, H. Lindstrom, E. Magnusson, A. Holmberg, A. Hagfeldt, J. Photochem. Photobiol. A: Chem. 148 (2002) 11.
[32] S.A. Haque, E. Palomares, B.M. Cho, A.N.M. Green, N. Hirata, D.R. Klug, J.R. Durrant, J. Am. Chem. Soc. 127 (2005) 3456.
[33] The thickness T of the shell WO_3 on the surface of TiO_2 was estimated by $T = (R/3) \times (W_{shell}/W_{core}) \times (\rho_{shell}/\rho_{core})$, where R is the median radius of a core TiO_2 particle, W_{shell} and W_{core} are the mass of shell WO_3 and core TiO_2 and ρ_{shell} and ρ_{core} are the density of the shell WO_3 and core TiO_2.